Article

AMPK phosphorylation of ACC2 is required for skeletal muscle fatty acid oxidation and insulin sensitivity in mice

Hayley M. O'Neill[1,2], James S. Lally[1], Sandra Galic[2], Melissa Thomas[3], Paymon D. Azizi[1], Morgan D. Fullerton[1], Brennan K. Smith[1,5], Thomas Pulinilkunnil[6], Zhiping Chen[2], M. Constantine Samaan[4], Sebastian B. Jorgensen[2,7], Jason R. B. Dyck[6], Graham P. Holloway[5], Thomas J. Hawke[3], Bryce J. van Denderen[2], Bruce E. Kemp[2], Gregory R. Steinberg[1,2]

1. Division of Endocrinology and Metabolism, Department of Medicine, HSC 4N63, McMaster University, 1280 Main St West, Hamilton, ON, Canada L8N 3Z5
2. St Vincent's Institute of Medical Research and Department of Medicine, University of Melbourne, Fitzroy, VIC, Australia
3. Department of Pathology and Molecular Medicine, McMaster University, Hamilton, ON, Canada
4. Department of Paediatrics, McMaster University, Hamilton, ON, Canada
[5]Department of Human Health and Nutritional Sciences, University of Guelph, Guelph, ON, Canada
[6]Cardiovascular Research Centre, Mazankowski Alberta Heart Institute, Department of Pediatrics, Faculty of Medicine and Dentistry, University of Alberta, Edmonton, AB, Canada
[7]Diabetes Research Unit, Novo Nordisk A/S, Maaloev, Denmark

Corresponding author
G. R. Steinberg, Division of Endocrinology and Metabolism, Department of Medicine, HSC 4N63, McMaster University, 1280 Main St West, Hamilton, ON, Canada L8N 3Z5
E-mail: gsteinberg@mcmaster.ca

Received: 12 February 2014 / Accepted: 2 May 2014

Abstract
Aims/hypothesis Obesity is characterised by lipid accumulation in skeletal muscle, which increases the risk of developing insulin resistance and type 2 diabetes. AMP-activated protein kinase (AMPK) is a sensor of cellular energy status and is activated in skeletal muscle by

exercise, hormones (leptin, adiponectin, IL-6) and pharmacological agents (5-amino-4-imidazolecarboxamide ribonucleoside [AICAR] and metformin). Phosphorylation of acetyl-CoA carboxylase 2 (ACC2) at S221 (S212 in mice) by AMPK reduces ACC activity and malonyl-CoA content but the importance of the AMPK–ACC2–malonyl-CoA pathway in controlling fatty acid metabolism and insulin sensitivity is not understood; therefore, we characterised *Acc2* S212A knock-in (ACC2 KI) mice.

Methods Whole-body and skeletal muscle fatty acid oxidation and insulin sensitivity were assessed in ACC2 KI mice and wild-type littermates.

Results ACC2 KI mice were resistant to increases in skeletal muscle fatty acid oxidation elicited by AICAR. These mice had normal adiposity and liver lipids but elevated contents of triacylglycerol and ceramide in skeletal muscle, which were associated with hyperinsulinaemia, glucose intolerance and skeletal muscle insulin resistance.

Conclusions/interpretation These findings indicate that the phosphorylation of ACC2 S212 is required for the maintenance of skeletal muscle lipid and glucose homeostasis.

Keywords

ACC2, AMPK, Fatty acid oxidation, Insulin resistance, Knock-in mice, Malonyl-CoA, Skeletal muscle

Abbreviations

2DG	2-Deoxyglucose
ACC	Acetyl-CoA carboxylase
ACC DKI	*Acc* double knock-in mice
ACC2 KI	*Acc2* S212A KI
AMPK β1β2 M-KO	Skeletal muscle-specific *Ampk* β1β2 KO
AICAR	5-Amino-4-imidazolecarboxamide ribonucleoside
AMPK	AMP-activated protein kinase
CPT-I	Carnitine palmitoyl transferase
Cyt	Cytochrome
DKI	Double KI
EDL	Extensor digitorum longus
GDR	Glucose disposal rate
HFD	High-fat diet

KI	Knock-in
KO	Knockout
OXPHOS	Proteins involved in oxidative phosphorylation
RQ	Respiratory quotient
TAG	Triacylglycerol
TBC1D 1 and 4	tre-2/USP6, BUB2, cdc16 domain family member 1 and 4
$\dot{V}CO_2$	Rate of CO_2 elimination
$\dot{V}O_2$	Rate of O_2 consumption
WT	Wild-type

Introduction

Skeletal muscle is the major site of insulin-stimulated glucose disposal (~ 80%); therefore, metabolic perturbations in this tissue have an important influence on whole-body glucose homeostasis. AMP-activated protein kinase (AMPK) is an evolutionarily conserved metabolic stress-sensing kinase that regulates cellular energy status by phosphorylating key substrates [1]. Consistent with its role as an energy sensor, skeletal muscle AMPK is rapidly activated in response to exercise and hormones, an effect associated with increases in fatty acid oxidation [2]. Fatty acid oxidation in skeletal muscle is regulated by carnitine palmitoyl transferase (CPT-I), which mediates the transport of long-chain fatty acids across the outer mitochondrial membrane by binding them to carnitine. CPT-I activity is inhibited by malonyl-CoA, which is produced following carboxylation of acetyl-CoA by acetyl-CoA carboxylase (ACC). ACC exists as two isoforms, ACC1 and ACC2 [3]. Liver, brown and white adipose and the brain contain predominantly ACC1 with low amounts of ACC2, while skeletal and cardiac muscles contain almost exclusively ACC2 [3, 4]. ACC1 and ACC2 are distinguished by an N-terminal extension of 146 amino acids in ACC2 that is thought to localise this isoform to the outer mitochondrial membrane [5] thus facilitating the regulation of fatty acid oxidation by malonyl-CoA inhibition of CPT-I. Initial reports that ACC2 null (knockout [KO]) mice had accelerated fatty acid oxidation and enhanced insulin sensitivity appeared to fit with ACC2 having an important role in regulating insulin sensitivity [6, 7]. However, two independent reports have recently questioned these findings: Hoehn et al [8] and Olson et al [9] found no change in body mass or insulin sensitivity of whole-body and skeletal muscle-specific ACC2 KO mice, respectively. Thus the role of ACC2 in controlling body mass and adiposity, skeletal muscle fatty acid oxidation and insulin sensitivity is currently unclear.

Genetic mouse models have been utilised to better understand the role of AMPK in controlling skeletal muscle fatty acid oxidation. Studies in *Ampk* (also known as *Prkaa2*) whole-body α2 and β2 KO, skeletal muscle-specific α2 kinase dead (KD) and skeletal muscle-specific *Ampk* β1β2 KO (AMPK β1β2 M-KO) mice, which all have dramatic reductions in skeletal muscle AMPK activity, have found that fatty acid oxidation is not impaired [10-13]. A caveat of these models is that a small degree of ACC phosphorylation is still present, which may be sufficient to inhibit ACC activity and increase fatty acid oxidation. However, changes in substrate use cannot be viewed in isolation because AMPK has multiple substrates that have an impact on carbohydrate and fatty acid metabolism [1]. In

addition, compensatory regulation of AMPK-independent pathways, like those involving sirtuin 1 and tre-1/USP6, BUB2, cdc 16 domain family member 1 (TBC1D1), could increase fatty acid oxidation [14].

To alleviate these concerns we have recently characterised mice harbouring targeted knock-in (Ser-Ala) mutations at both S79 and S212 AMPK phosphorylation sites on ACC1 and ACC2, respectively (named *Acc* double knock-in mice [ACC DKI]) [15]. Tissues from ACC DKI mice have increased ACC activity and malonyl-CoA, increased rates of liver lipogenesis and reduced fatty acid oxidation, contributing to a fatty liver. ACC DKI mice also have reduced rates of skeletal muscle fatty acid oxidation and develop modest impairments in muscle insulin sensitivity. Despite these data indicating that AMPK phosphorylation of both ACC1 and ACC2 is critical for controlling insulin sensitivity, the importance of the ACC2 isoform in controlling whole-body or skeletal muscle fatty acid oxidation and insulin sensitivity has not been tested. This is especially relevant for a number of reasons: (1) there are discrepancies regarding the importance of ACC2 in controlling skeletal muscle insulin sensitivity [6-9]; (2) ACC1 may be able to compensate for ACC2 function in the control of skeletal muscle fatty acid oxidation [9]; (3) it is not currently known whether pharmacological activators of AMPK that increase skeletal muscle fatty acid oxidation (e.g. 5-amino-4-imidazolecarboxamide ribonucleoside [AICAR]) mediate their effects through the AMPK–ACC signalling pathway.

To specifically assess the contribution of ACC2 S212 phosphorylation in regulating fatty acid oxidation and insulin sensitivity we characterised *Acc2* S212A KI (ACC2 KI) mice. We found that ACC2 KI mice tended to have reduced fatty acid oxidation rates in skeletal muscle and, importantly, this was not increased by AICAR treatment. Consistent with these findings ACC2 KI mice fed a control chow diet had increased lipid deposition in skeletal muscle and developed insulin resistance, suggesting that ACC2 S212 phosphorylation is required for the maintenance of not only skeletal muscle lipid homeostasis but also glucose metabolism in lean healthy mice. However, on an obesity-promoting high-fat diet (HFD) ACC2 KI mice were indistinguishable from their wild-type (WT) littermates suggesting that the HFD overwhelmed the genotype differences observed in chow-fed mice.

Methods

Animal experiments ACC2 KI mice were generated and housed as described [15]. Male mice at 6 weeks of age were maintained on a chow diet (17% kJ fat; diet 8640, Harlan Teklad,

Madison, WI, USA) or an HFD (SF04-027; Specialty Feeds, Perth, WA, Australia) for 12 weeks and had free access to food and water. All animal procedures were approved by the St Vincent's Hospital Animal Ethics Committee and McMaster University Animal Ethics Committee. Fed and overnight-fasted (12 h) blood was collected via submandibular bleed and serum was stored at –80°C before analyses [12].

Basal metabolism cage experiments and the calculation of substrate utilisation were performed as described [12, 16]. Palmitate oxidation was measured in isolated extensor digitorium longus (EDL) muscle, with or without AICAR (2 mmol/l) [10]. Hyperinsulinaemic–euglycaemic clamps were performed as described [15, 17]. 2-Deoxyglucose (2DG) uptake was determined in isolated soleus and EDL muscles treated with vehicle or submaximal concentration of insulin (400 μU/ml) . See electronic supplementary material (ESM) Methods for details.

Analytical methods For western blotting, muscle lysates were prepared and antibodies used as described. The mRNA expression of *Acc1, Acc2, Tnf, Il1b, Il6, Kc* (also known as *Cxcl1*), *Ccl2* and *Il10* was determined in quadriceps muscle. Adipocyte size was determined in white epididymal adipose sections that had been fixed in formalin, embedded in paraffin and stained with haematoxylin and eosin [18]. Citrate synthase activity was determined as described . The activity of succinate dehydrogenase and cytochrome (cyt) c oxidase and the assessment of fibre-type distribution were performed as described in the supplementary methods. Muscle glycogen content was determined as glycosyl units after acid hydrolysis [19]. Triacylglycerol (TAG) was extracted [20] and lipidomics performed. To determine the sensitivity of CPT-I to malonyl-CoA, saponin permeabilised fibres were prepared as described [21, 22]. See ESM Methods for details.

Statistics Unless otherwise noted, data were expressed as means ± SEM. Results were analysed using Student's *t* test, paired *t* test or ANOVA procedures, where appropriate, using GraphPad Prism version 5.01 for Windows, GraphPad Software, La Jolla, CA, USA, www.graphpad.com. Significance was accepted at $p < 0.05$.

Results

ACC2 S212 phosphorylation is required for controlling muscle fatty acid oxidation in response to AICAR ACC2 KI mice had no detectable ACC2 S212 phosphorylation either

basally or following treatment with AICAR, confirming successful S212 mutation in ACC2 KI mice and that ACC2 is the only detectable ACC isoform present in skeletal muscle (Fig. 1a). The ACC2 KI mutation did not alter *Acc1* or *Acc2* mRNA expression, ACC1 or ACC2 protein expression (ESM Fig. 1 a, b) or AMPK α2 activity (Fig. 1b). Malonyl-CoA decarboxylase, which plays a reciprocal role to ACC in the regulation of malonyl-CoA production [23-25] and is downregulated in ACC2 M-KO mice [9], was unchanged in skeletal muscle of ACC2 KI mice (ESM Fig. 1c).

We next measured fatty acid oxidation in skeletal muscle from WT and ACC2 KI mice treated with or without 2 mmol/l AICAR. Fatty acid oxidation tended to be lower in isolated EDL muscles from ACC2 KI mice (– 24%; $p < 0.06$) and was increased in isolated EDL muscles from WT but not ACC2 KI mice in response to AICAR (Fig. 1c). These data highlight the importance of ACC2 S212 phosphorylation in controlling skeletal muscle fatty acid oxidation with the pharmacological AMPK activator AICAR. To investigate whether these differences in muscle fatty acid oxidation have an impact on whole-body rates of substrate use we completed experiments in metabolism cages wherein mice were injected with either saline or AICAR. There was no significant difference in oxygen consumption ($\dot{V}O_2$) or CO_2 elimination ($\dot{V}CO_2$) between genotypes or treatments; however, the respiratory quotient (RQ) was significantly reduced in WT but not ACC2 KI mice (ESM Table 1). The drop in RQ indicates a greater reliance on fatty acid substrates in WT but not ACC2 KI mice following AICAR injection (Fig. 1d), a finding consistent with changes in ACC phosphorylation (Fig. 1e). These data indicate that pharmacological activation of AMPK by AICAR increases whole-body rates of fatty acid oxidation through the phosphorylation of ACC2 S212.

ACC2 KI mice have normal appetite and energy expenditure and do not develop obesity when fed a control chow diet We found that at 18 weeks of age body mass, adiposity and adipocyte size were comparable between WT and ACC2 KI mice (Fig. 2 a, b). Similarly, oxygen consumption, activity levels and food intake were not altered in ACC2 KI mice (Table 1), indicating that phosphorylation of ACC2 is not critical for controlling whole-body energy expenditure or intake.

ACC2 S212 phosphorylation is required for preventing ectopic lipid accumulation in skeletal muscle Despite similar adiposity, body mass and energy expenditure, modest changes in

skeletal muscle fatty acid oxidation would be anticipated to alter skeletal muscle lipid levels over time. Consistent with this hypothesis, we found that ACC2 KI mice had a 76% increase in skeletal muscle TAG (Fig. 2c). There were no differences in liver TAG (Fig. 2c), which is reliant on both ACC1 S79 and ACC2 S212 phosphorylation [15]. Muscle lipidomics found that this increase was not confined to TAG, as C16:0, C18:0 and C20:0 ceramides were also increased in ACC2 KI muscle (Fig. 2d). Consistent with a shift towards lower rates of skeletal muscle fatty acid oxidation, ACC2 KI mice had reduced muscle glycogen, indicative of a greater reliance on carbohydrate oxidation (Fig. 2e), whereas liver glycogen was not changed (Fig. 2e). These data demonstrate that ACC2 S212 phosphorylation is essential for maintaining skeletal muscle lipid homeostasis.

Lack of ACC2 S212 phosphorylation does not adversely alter mitochondrial function in skeletal muscle Mitochondrial dysfunction or reduced mitochondrial biogenesis and density can also lead to a decrease in fatty acid oxidation and subsequent accumulation of bioactive lipids including ceramides [26]; therefore, we assessed these variables. We found that citrate synthase and succinate dehydrogenase activity, and expression of proteins involved in oxidative phosphorylation (OXPHOS), were not different in ACC2 KI mice (Fig. 3 a–e). This was despite an increase in cyt c oxidase activity and a modest oxidative fibre-type shift (type IIb to type a/x myosin heavy chain isoforms) (Fig. 3 f, g). In addition, maximal mitochondrial respiratory chain complex function was normal in the presence of various substrates, including palmitoyl-CoA and palmitate (Fig. 3h), indicating that mitochondrial function was intact. Altered CPT-I sensitivity to malonyl-CoA has been reported [27-29] but there was no difference in palmitoyl-CoA respiration rates and IC_{50} for malonyl-CoA between permeabilised muscle fibres of WT and ACC2 KI mice (Fig. 4). Collectively these data indicate that the ACC2 KI mutation results in reduced fatty acid oxidation rates independent of intrinsic changes in mitochondrial function.

ACC2 S212 phosphorylation is required for the maintenance of skeletal muscle insulin sensitivity Elevated skeletal muscle ceramides can contribute to the development of insulin resistance [30]. ACC2 KI mice had fasting hyperinsulinaemia (Fig. 5a) and developed modest whole-body glucose and insulin intolerance (Fig. 5 b, c). We subsequently performed hyperinsulinaemic–euglycaemic clamps (ESM Table 2). During the clamp ACC2 KI mice had a lower glucose infusion rate (GINF) (Fig. 5d) and this was due to a reduced glucose disposal rate (GDR) (Fig. 5e). Hepatic glucose production and per cent suppression of hepatic

glucose production were not altered indicating that ACC2 KI mice had normal liver insulin sensitivity (ESM Table 2). Serum insulin during the clamp was similar between genotypes (ESM Table 2). To examine whether adipose tissue or skeletal muscle contributed to impaired insulin-stimulated GDR we measured insulin-stimulated 2DG clearance following the clamp and found that ACC2 KI mice had a strong tendency for reduced skeletal muscle 2DG clearance ($p = 0.06$, Fig. 5f). There was no difference in adipose tissue 2DG clearance (ESM Table 2). Similar observations of reduced insulin-stimulated glucose uptake were observed in soleus and EDL muscles isolated from ACC2 KI mice and treated with insulin ex vivo suggesting that the defect in insulin action was intrinsic to skeletal muscle and not due to a change in circulating factors (Fig. 5g). These data indicate that ACC2 S212 phosphorylation is important for preventing insulin resistance in skeletal muscle but not liver or adipose tissue.

To investigate the mechanisms contributing to skeletal muscle insulin resistance in ACC2 KI mice we examined insulin-signal transduction. We found that, consistent with recent reports indicating that ceramide-induced insulin resistance in skeletal muscle is downstream of canonical insulin signalling [31], Akt and TBC1D4/TBC1D1 phosphorylation were unaltered in insulin-stimulated muscles (gastrocnemius muscle following the clamp and isolated soleus and EDL muscles treated with or without 400 μU/ml insulin) of ACC2 KI mice compared with WT controls (Fig. 6 a–d). Reduced muscle insulin sensitivity in ACC2 KI mice also appeared to be independent of changes in GLUT4 expression and muscle inflammation (Fig. 6 e, f). These data suggest that control of muscle insulin resistance is likely downstream of TBC1D4 and may involve plasma membrane remodelling and GLUT4 trafficking as proposed [32].

ACC2 S212 phosphorylation does not exacerbate the development of HFD-induced obesity or insulin resistance We also examined the effects of an HFD and found that after 12 weeks WT and ACC2 KI mice had increased body mass and adiposity as well as increased serum leptin levels compared with chow-fed controls but there were no differences between genotypes (Fig. 7a and ESM Table 3). We found that while, as expected, the HFD reduced the RQ compared with chow controls there were no differences between genotypes indicating that ACC2 phosphorylation is not required for the upregulation of fatty acid oxidation in response to increased substrate availability (Table 1). There were also no genotypic differences in food intake, activity levels or oxygen consumption (Table 1). In contrast to the genotype effect observed in chow-fed mice, there were no differences in serum insulin or NEFA between WT

and ACC2 KI mice fed an HFD (Fig. 7b). Similarly, neither insulin sensitivity nor glucose tolerance was different between ACC2 KI and WT mice on an HFD (Fig. 7 c, d). Consistent with comparable insulin sensitivity when fed the HFD, we found that skeletal muscle TAG and insulin-stimulated glucose uptake were comparable between genotypes (Fig. 7 e, f).

Discussion

ACC1 and ACC2 have distinct structures as well as cellular and tissue specific localisation but our understanding of their enzymatic control is almost entirely based on studies involving ACC1 [33-36]. With the discovery of ACC2 and its primary localisation to the outer mitochondrial membrane in skeletal muscle [5], it was assumed that phosphorylation of ACC2 S212 by AMPK regulated enzyme activity in a manner similar to ACC1 and that this may be important for controlling skeletal muscle fatty acid oxidation. While associations between AICAR-stimulated ACC2 phosphorylation and fatty acid oxidation have been reported [8, 10, 37-39], in the current study we provide direct genetic evidence establishing that AICAR-induced increases in fatty acid oxidation are dependent on ACC2 S212 phosphorylation (Fig. 1). Importantly, the phenotypic differences in fatty acid oxidation indicate that ACC2 S212 phosphorylation is the primary point of AMPK regulation of skeletal muscle fatty acid oxidation.

The phosphorylation of ACC2 S212 is increased in skeletal muscle in response to multiple circulating hormones that increase fatty acid oxidation, reduce obesity and improve insulin sensitivity (for review see [40]); therefore, we hypothesised that ACC2 KI mice might develop obesity and insulin resistance. However, ACC2 KI mice did not become obese despite having reduced rates of fatty acid oxidation in skeletal muscle. An important aspect of our study is that while resting muscle contributes ~ 20% to whole-body resting energy expenditure we did not detect differences in the RQ of ACC2 KI mice. We have found that the ACC2 KI mutation on its own does not have an impact on fatty acid oxidation in tissues expressing the ACC1 isoform, such as the liver [15]; therefore, detecting small reductions in basal fatty acid oxidation (~ 15%) in muscle of the ACC2 KI mice would involve detecting a 2–3% change in RQ, which is likely below the limits of detection of indirect calorimetry. Importantly, even if there was a detectable reduction in whole-body rates of fatty acid oxidation, this would not be sufficient to promote the development of obesity without a decrease in whole-body energy expenditure as previously described [8].

We found that reduction in skeletal muscle fatty acid oxidation was associated with an increase in muscle TAG, equivalent to that in an obese mouse fed an HFD for 12 weeks. In

contrast, ACC2 KI mice had normal levels of liver lipids. It is now well accepted that intramuscular TAG is unlikely to cause insulin resistance, but instead serves as a protective mechanism to sequester reactive lipids [41, 42]. Rather, spillover from the intramuscular TAG pool into ceramides plays an import role in the development of skeletal muscle insulin resistance [43-45] as ceramides compromise membrane dynamics resulting in improper GLUT4 insertion. In agreement with these findings, ACC2 KI mice had elevated skeletal muscle ceramides, which was associated with skeletal muscle insulin resistance that was independent of defects in insulin-signal transduction, GLUT4 expression and muscle inflammation. This is consistent with recent reports demonstrating that control of lipid-induced insulin resistance is downstream of TBC1D4 signalling and may involve actin remodelling [31, 32]. Consistent with the development of skeletal muscle insulin resistance, ACC2 KI mice also developed whole-body hyperinsulinaemia and impaired whole-body glucose tolerance and insulin sensitivity. So a key question is what was the source of substrate that ACC2 KI mice were using in order to provide energy if both fatty acid oxidation and insulin-stimulated glucose uptake were reduced? We speculate that under conditions of reduced glucose uptake and reduced fatty acid oxidation most of the glucose that is taken up is channelled to oxidation, leaving less available for storage as glycogen. This idea is supported by lower glycogen levels in skeletal muscle of ACC2 KI mice.

We also assessed insulin sensitivity in ACC2 KI mice when metabolically challenged with an HFD for 12 weeks. Interestingly, the ACC2 KI mutation had no effect on insulin sensitivity when mice were fed the HFD. This may be due to reduced muscle AMPK and ACC phosphorylation, which is common in obese mice [46] and would in turn be expected to minimise the genotype differences. Additionally, it is known that pyruvate dehydrogenase kinase 4, a key enzyme involved in switching glucose to fatty acid oxidation by inhibiting pyruvate dehydrogenase activity (and glucose oxidation) [47], is upregulated in response to an HFD [48, 49]. Further studies investigating AMPK–ACC2-independent mechanisms regulating fatty acid oxidation under high fatty acid availability are warranted.

In conclusion, we demonstrate that S212 phosphorylation of ACC2 is essential for regulating not only skeletal muscle fatty acid oxidation but also insulin sensitivity. As skeletal muscle ACC2 phosphorylation may be reduced in obesity and type 2 diabetes [50], our studies suggest that therapies aimed at restoring or mimicking ACC2 phosphorylation may represent an important therapeutic strategy for restoring insulin sensitivity.

Funding

These studies were supported by grants and fellowships from the Australian Research Council and CSIRO (BEK), National Health and Medical Research Council (BEK, GRS, BJvD), the Canadian Diabetes Association (GRS) and the Canadian Institutes of Health Research (CIHR) (GRS). Support in part was received from the Victorian Government's OIS Program (BEK) and Canadian Foundation for Innovation (GRS). MDF is a CIHR Banting Postdoctoral Fellow and GRS holds a Canada Research Chair in Metabolism and Obesity.

Contribution statement

HMO and GRS designed experiments and wrote manuscript. GRS, BEK and SBJ provided funding for the project and revised the manuscript. HMO performed the majority of experiments. JSL, SG, MT, PDA, MDF, BKS, TP, ZC, BJvD, MCS, SBJ, JRBD, GPH and TJH designed and performed experiments and revised the manuscript. All authors approved the final version of the manuscript. GRS is responsible for the integrity of the work as a whole.

Duality of interest

The authors declare that there is no duality of interest associated with this manuscript.

References

[1] Steinberg GR, Kemp BE (2009) AMPK in Health and Disease. Physiol Rev 89: 1025-1078

[2] Steinberg GR, Jorgensen SB (2007) The AMP-activated protein kinase: role in regulation of skeletal muscle metabolism and insulin sensitivity. Mini reviews in medicinal chemistry 7: 519-526

[3] Abu-Elheiga L, Jayakumar A, Baldini A, Chirala SS, Wakil SJ (1995) Human acetyl-CoA carboxylase: characterization, molecular cloning, and evidence for two isoforms. Proc Natl Acad Sci U S A 92: 4011-4015

[4] Iverson AJ, Bianchi A, Nordlund AC, Witters LA (1990) Immunological analysis of acetyl-CoA carboxylase mass, tissue distribution and subunit composition. Biochem J 269: 365-371

[5] Abu-Elheiga L, Brinkley WR, Zhong L, Chirala SS, Woldegiorgis G, Wakil SJ (2000) The subcellular localization of acetyl-CoA carboxylase 2. Proc Natl Acad Sci U S A 97: 1444-1449

[6] Choi CS, Savage DB, Abu-Elheiga L, et al. (2007) Continuous fat oxidation in acetyl-CoA carboxylase 2 knockout mice increases total energy expenditure, reduces fat mass, and improves insulin sensitivity. Proc Natl Acad Sci U S A 104: 16480-16485

[7] Abu-Elheiga L, Oh W, Kordari P, Wakil SJ (2003) Acetyl-CoA carboxylase 2 mutant mice are protected against obesity and diabetes induced by high-fat/high-carbohydrate diets. Proc Natl Acad Sci U S A 100: 10207-10212

[8] Hoehn KL, Turner N, Swarbrick MM, et al. (2010) Acute or chronic upregulation of mitochondrial fatty acid oxidation has no net effect on whole-body energy expenditure or adiposity. Cell Metab 11: 70-76

[9] Olson DP, Pulinilkunnil T, Cline GW, Shulman GI, Lowell BB (2010) Gene knockout of Acc2 has little effect on body weight, fat mass, or food intake. Proc Natl Acad Sci U S A 107: 7598-7603

[10] Dzamko N, Schertzer JD, Ryall JG, et al. (2008) AMPK-independent pathways regulate skeletal muscle fatty acid oxidation. J Physiol 586: 5819-5831

[11] Jeppesen J, Maarbjerg SJ, Jordy AB, et al. (2013) LKB1 Regulates Lipid Oxidation During Exercise Independently of AMPK. Diabetes

[12] O'Neill HM, Maarbjerg SJ, Crane JD, et al. (2011) AMP-activated protein kinase (AMPK) beta1beta2 muscle null mice reveal an essential role for AMPK in maintaining mitochondrial content and glucose uptake during exercise. Proc Natl Acad Sci U S A 108: 16092-16097

[13] Steinberg GR, O'Neill HM, Dzamko NL, et al. (2010) Whole-body deletion of AMPK β2 reduces muscle AMPK and exercise capacity. J Biol Chem 285: 37198-37209

[14] Lee CW, Wong LL, Tse EY, et al. (2012) AMPK promotes p53 acetylation via phosphorylation and inactivation of SIRT1 in liver cancer cells. Cancer research 72: 4394-4404

[15] Fullerton MD, Galic S, Marcinko K, et al. (2013) Single phosphorylation sites in Acc1 and Acc2 regulate lipid homeostasis and the insulin-sensitizing effects of metformin. Nat Med 19: 1649-1654

[16] Hawley SA, Fullerton MD, Ross FA, et al. (2012) The ancient drug salicylate directly activates AMP-activated protein kinase. Science 336: 918-922

[17] Galic S, Fullerton MD, Schertzer JD, et al. (2011) Hematopoietic AMPK beta1 reduces mouse adipose tissue macrophage inflammation and insulin resistance in obesity. J Clin Invest 121: 4903-4915

[18] Palanivel R, Fullerton MD, Galic S, et al. (2012) Reduced Socs3 expression in adipose tissue protects female mice against obesity-induced insulin resistance. Diabetologia 55: 3083-3093

[19] Passonneau JV, Gatfield PD, Schulz DW, Lowry OH (1967) An enzymic method for measurement of glycogen. Anal Biochem 19: 315-326

[20] Watt MJ, Dzamko N, Thomas WG, et al. (2006) CNTF reverses obesity-induced insulin resistance by activating skeletal muscle AMPK. Nature medicine 12: 541-548

[21] Anderson EJ, Lustig ME, Boyle KE, et al. (2009) Mitochondrial H2O2 emission and cellular redox state link excess fat intake to insulin resistance in both rodents and humans. J Clin Invest 119: 573-581

[22] Smith BK, Jain SS, Rimbaud S, et al. (2011) FAT/CD36 is located on the outer mitochondrial membrane, upstream of long-chain acyl-CoA synthetase, and regulates palmitate oxidation. Biochem J 437: 125-134

[23] Bouzakri K, Austin R, Rune A, et al. (2008) Malonyl CoenzymeA decarboxylase regulates lipid and glucose metabolism in human skeletal muscle. Diabetes 57: 1508-1516

[24] Joly E, Bendayan M, Roduit R, Saha AK, Ruderman NB, Prentki M (2005) Malonyl-CoA decarboxylase is present in the cytosolic, mitochondrial and peroxisomal compartments of rat hepatocytes. FEBS Lett 579: 6581-6586

[25] Park H, Kaushik VK, Constant S, et al. (2002) Coordinate regulation of malonyl-CoA decarboxylase, sn-glycerol-3-phosphate acyltransferase, and acetyl-CoA carboxylase by AMP-activated protein kinase in rat tissues in response to exercise. J Biol Chem 277: 32571-32577

[26] Lowell BB, Shulman GI (2005) Mitochondrial dysfunction and type 2 diabetes. Science 307: 384-387

[27] Kerner J, Distler AM, Minkler P, Parland W, Peterman SM, Hoppel CL (2004) Phosphorylation of rat liver mitochondrial carnitine palmitoyltransferase-I: effect on the kinetic properties of the enzyme. J Biol Chem 279: 41104-41113

[28] Bezaire V, Heigenhauser GJ, Spriet LL (2004) Regulation of CPT I activity in intermyofibrillar and subsarcolemmal mitochondria from human and rat skeletal muscle. Am J Physiol Endocrinol Metab 286: E85-91

[29] Holloway GP, Bezaire V, Heigenhauser GJ, et al. (2006) Mitochondrial long chain fatty acid oxidation, fatty acid translocase/CD36 content and carnitine palmitoyltransferase I activity in human skeletal muscle during aerobic exercise. J Physiol 571: 201-210

[30] Holland WL, Brozinick JT, Wang LP, et al. (2007) Inhibition of ceramide synthesis ameliorates glucocorticoid-, saturated-fat-, and obesity-induced insulin resistance. Cell Metab 5: 167-179

[31] Hoehn KL, Hohnen-Behrens C, Cederberg A, et al. (2008) IRS1-independent defects define major nodes of insulin resistance. Cell Metab 7: 421-433

[32] JeBailey L, Wanono O, Niu W, Roessler J, Rudich A, Klip A (2007) Ceramide- and oxidant-induced insulin resistance involve loss of insulin-dependent Rac-activation and actin remodeling in muscle cells. Diabetes 56: 394-403

[33] Davies SP, Sim AT, Hardie DG (1990) Location and function of three sites phosphorylated on rat acetyl-CoA carboxylase by the AMP-activated protein kinase. Eur J Biochem 187: 183-190

[34] Munday MR, Campbell DG, Carling D, Hardie DG (1988) Identification by amino acid sequencing of three major regulatory phosphorylation sites on rat acetyl-CoA carboxylase. Eur J Biochem 175: 331-338

[35] Ha J, Daniel S, Broyles SS, Kim KH (1994) Critical phosphorylation sites for acetyl-CoA carboxylase activity. J Biol Chem 269: 22162-22168

[36] Corton JM, Gillespie JG, Hawley SA, Hardie DG (1995) 5-aminoimidazole-4-carboxamide ribonucleoside. A specific method for activating AMP-activated protein kinase in intact cells? Eur J Biochem 229: 558-565

[37] Thomson DM, Brown JD, Fillmore N, et al. (2007) LKB1 and the regulation of malonyl-CoA and fatty acid oxidation in muscle. Am J Physiol Endocrinol Metab 293: E1572-1579

[38] Kaushik VK, Young ME, Dean DJ, Kurowski TG, Saha AK, Ruderman NB (2001) Regulation of fatty acid oxidation and glucose metabolism in rat soleus muscle: effects of AICAR. Am J Physiol Endocrinol Metab 281: E335-340

[39] Merrill GF, Kurth EJ, Hardie DG, Winder WW (1997) AICA riboside increases AMP-activated protein kinase, fatty acid oxidation, and glucose uptake in rat muscle. Am J Physiol 273: E1107-1112

[40] Dzamko NL, Steinberg GR (2009) AMPK-dependent hormonal regulation of whole-body energy metabolism. Acta Physiol (Oxf) 196: 115-127

[41] Schenk S, Horowitz JF (2007) Acute exercise increases triglyceride synthesis in skeletal muscle and prevents fatty acid-induced insulin resistance. J Clin Invest 117: 1690-1698

[42] Liu L, Zhang Y, Chen N, Shi X, Tsang B, Yu YH (2007) Upregulation of myocellular DGAT1 augments triglyceride synthesis in skeletal muscle and protects against fat-induced insulin resistance. J Clin Invest 117: 1679-1689

[43] Ussher JR, Koves TR, Cadete VJ, et al. (2010) Inhibition of de novo ceramide synthesis reverses diet-induced insulin resistance and enhances whole-body oxygen consumption. Diabetes 59: 2453-2464

[44] Pickersgill L, Litherland GJ, Greenberg AS, Walker M, Yeaman SJ (2007) Key role for ceramides in mediating insulin resistance in human muscle cells. J Biol Chem 282: 12583-12589

[45] Summers SA (2006) Ceramides in insulin resistance and lipotoxicity. Prog Lipid Res 45: 42-72

[46] Steinberg GR, Michell BJ, van Denderen BJ, et al. (2006) Tumor necrosis factor alpha-induced skeletal muscle insulin resistance involves suppression of AMP-kinase signaling. Cell Metab 4: 465-474

[47] Sugden MC, Howard RM, Munday MR, Holness MJ (1993) Mechanisms involved in the coordinate regulation of strategic enzymes of glucose metabolism. Adv Enzyme Regul 33: 71-95

[48] Holness MJ, Kraus A, Harris RA, Sugden MC (2000) Targeted upregulation of pyruvate dehydrogenase kinase (PDK)-4 in slow-twitch skeletal muscle underlies the stable modification of the regulatory characteristics of PDK induced by high-fat feeding. Diabetes 49: 775-781

[49] Jeoung NH, Harris RA (2008) Pyruvate dehydrogenase kinase-4 deficiency lowers blood glucose and improves glucose tolerance in diet-induced obese mice. Am J Physiol Endocrinol Metab 295: E46-54

[50] Bandyopadhyay GK, Yu JG, Ofrecio J, Olefsky JM (2006) Increased malonyl-CoA levels in muscle from obese and type 2 diabetic subjects lead to decreased fatty acid oxidation and increased lipogenesis; thiazolidinedione treatment reverses these defects. Diabetes 55: 2277-2285

Table 1 Resting metabolic variables of WT and ACC2 KI mice fed a chow diet or HFD

Variable	Chow diet		HFD	
	WT	ACC2 KI	WT	ACC2 KI
$\dot{V}O_2$ (ml kg^{-1} h^{-1})				
Dark	2,917 ± 28.74	2,945 ± 33.92	2,111 ± 26.59	2,290 ± 22.80
Light	2,214 ± 20.51	2,207 ± 23.77	1,759 ± 16.81	1,829 ± 17.28
RQ ($\dot{V}CO_2/\dot{V}O_2$)				
Dark	0.91 ± 0.00	0.92 ± 0.00	0.83 ± 0.00	0.81 ± 0.00
Light	0.89 ± 0.00	0.89 ± 0.00	0.84 ± 0.00	0.83 ± 0.00
Activity (XAMB beam breaks/12 h)				
Dark	31,641 ± 51.24	34,280 ± 68.18	16,688 ± 5.23	15,536 ± 6.91
Light	5,588 ± 14.29	6,519 ± 18.24	2,740 ± 74.27	2,981 ± 85.59
Food intake (g)				
Dark	1.69 ± 0.00	1.65 ± 0.00	1.31 ± 0.10	1.30 ± 0.09
Light	1.03 ± 0.00	1.10 ± 0.00	0.87 ± 0.11	1.02 ± 0.11

Data are means ± SEM, *n*=8

$\dot{V}O_2$, RQ, food intake and spontaneous activity levels (ambulatory activity [beam breaks]) across the *x*-axis of metabolic cages (XAMB beam breaks/12 h) over 72 h data were analysed for light (07:00–19:00 hours) and dark cycles (19:00–07:00 hours). Mice had free access to food and water

None of the variables differ between the ACC2 KI mice and the WT littermates

Figure legends

Fig. 1 ACC2 KI mice have reduced fatty acid oxidation. (**a**–**c**) ACC2 S212 phosphorylation relative to total ACC expression (**a**), AMPK α2 activity (**b**) and palmitate oxidation (**c**) in isolated EDL muscles treated ex vivo with or without AICAR (2 mmol/l). (**d**, **e**) Whole-body percentage fatty acid utilisation (**d**) and ACC2 S212 phosphorylation (**e**) relative to total ACC in gastrocnemius muscle following intraperitoneal injection of mice with saline or AICAR (0.5 g/kg body weight). Black bars, WT; white bars, ACC2 KI; ND, not detectable. Data are means ± SEM, n=6–8. *p<0.05 and ***p<0.001 and $^{\ddagger}p$=0.06 vs WT littermates; $^{\dagger}p$<0.05, $^{\dagger\dagger}p$<0.01 and $^{\dagger\dagger\dagger}p$<0.001 vs basal, same genotype

Fig. 2 Lipids are increased in ACC2 KI skeletal muscle. (**a**, **b**) Body (left y-axis) and white epididymal fat pad (WAT) mass (right y-axis) (**a**) and white adipose tissue cell size (area) (**b**) in 18-week-old chow-fed mice. (**c**) TAG in gastrocnemius muscle and liver, expressed as μg glycerol/mg tissue. (**d**) Ceramides (Cer) in tibialis anterior muscle. (**e**) Glycogen contents in gastrocnemius muscle (left y-axis) and liver (right y-axis), expressed as μg glycosyl units/mg tissue. Black bars, WT; white bars, ACC2 KI. Data are means ± SEM, n=8–14. *p<0.05 and ***p<0.001 vs WT littermates

Fig. 3 Muscle oxidative capacity is maintained in ACC2 KI mice. (**a**) Citrate synthase (Cs) activity in quadriceps muscle. (**b**) Succinate dehydrogenase activity in tibialis anterior (TA) muscle. (**c**–**e**) OXPHOS protein expression in soleus (**c**), EDL(**d**) and quadriceps (**e**) muscle. (**f**) Cyt c oxidase activity in TA. (**g**) Fibre-type distribution of myosin heavy chain isoforms in TA. (**h**) Mitochondrial respiratory chain complex function in permeabilised fibres isolated from gastrocnemius muscle. GM, glutamate + malate (state IV); GMD, glutamate + malate + ADP (state III); GMDc, glutatmate + malate + ADP + cyt c; GMDcS, glutamate + malate + ADP + cyt c + succinate. Black bars, WT; white bars, ACC2 KI. Data are means ± SEM (n=5 TA; n=8 Cs and OXPHOS; n=4 permeabilised fibres). *p<0.05 and $^{\ddagger}p$=0.07 vs WT littermates. d/w, dry weight

Fig. 4 CPT-I sensitivity to malonyl-CoA in permeabilised muscle fibres. (**a**) Palmitoyl-CoA (P.CoA) respiration rates in permeabilised fibres isolated from gastrocnemius muscle of WT (black squares) and ACC2 KI (white squares) mice in response to varying concentrations of

malonyl-CoA. (**b**) IC_{50} for malonyl-CoA. Data are means ± SEM, *n*=4. $\dot{V}_{max}$, maximal rate of respiration

Fig. 5 ACC2 KI mice have impaired insulin sensitivity. (**a**) Fasting (12 h) serum insulin. (**b**, **c**) Glucose (1 g/kg) (**b**) and insulin (0.6 U/kg) (**c**) tolerance tests and AUC (insets). (**d**, **e**) Glucose infusion rate (GINF) over time (**d**) and GDR during hyperinsulinaemic–euglycaemic clamp (**e**). (**f**) Insulin-stimulated 2DG uptake in gastrocnemius muscle following the clamp. (**g**) 2DG uptake in isolated soleus and EDL muscles treated ex vivo with or without insulin (400 μU/ml) (B, basal; Ins, insulin). Black bars and squares, WT; white bars and squares, ACC2 KI. Data are means ± SEM, *n*=8. **p*<0.05, ****p*<0.001 and $^{\ddagger}p$=0.06 vs WT littermates; $^{\dagger\dagger\dagger}p$<0.001 vs basal, same genotype

Fig. 6 Canonical insulin signalling is normal in ACC2 KI muscle. (**a**–**c**) Akt S473 (**a**) and T308 (**b**) and TBC1D4/1 T642/596 phosphorylation (**c**) in isolated soleus and EDL muscles treated ex vivo with or with insulin (400 μU/ml) (B, basal; Ins, insulin). (**d**) Insulin-stimulated Akt T308 phosphorylation in gastrocnemius muscle following completion of the hyperinsulinaemic–euglycaemic clamp. (**e**) GLUT4 expression in soleus and EDL muscles. (**f**) mRNA expression of inflammatory cytokines/chemokines in gastrocnemius muscle. Black bars, WT; white bars, ACC2 KI. Data are means ± SEM, *n*=8–16. $^{\dagger\dagger\dagger}p$<0.001 and $^{\ddagger}p$=0.09 vs basal, same genotype

Fig. 7 ACC2 KI mice fed an HFD have similar insulin sensitivity to WT controls. (**a**, **b**) Body and white epididymal fat pad (WAT) mass (**a**) and fasting serum NEFA and insulin (**b**) in mice after 12 weeks of HFD. (**c**, **d**) Glucose (1 g/kg) (**c**) and insulin (0.66 U/kg) (**d**) tolerance tests and AUC (insets). (**e**) TAG in gastrocnemius muscle and liver. (**f**) 2DG uptake in isolated soleus and EDL muscles treated ex vivo with or without insulin (400 μU/ml) (B, basal; Ins, insulin). Black bars, WT; white bars, ACC2 KI. Data are means ± SEM, *n*=8. $^{\dagger}p$<0.05 and $^{\dagger\dagger\dagger}p$<0.001 vs basal, same genotype

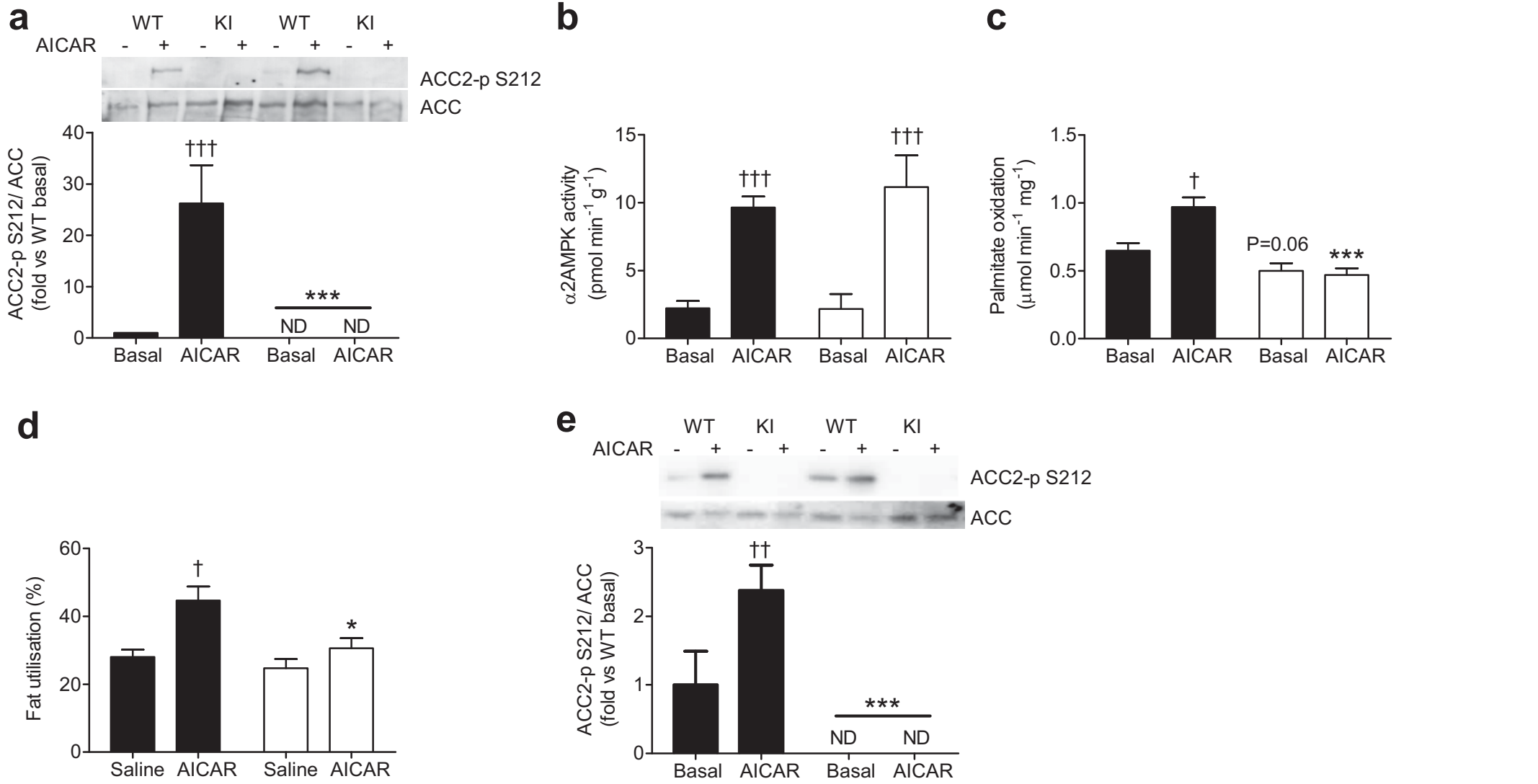
a
WT
KI
WT
KI
AICAR
- + - + - + - +
ACC2-p S212
ACC
ACC2-p S212/ ACC
(fold vs WT basal)
40
30
20
10
0
†††
***
ND
ND
Basal
AICAR
Basal
AICAR
b
α2AMPK activity
(pmol min-1 g-1)
15
10
5
0
†††
†††
Basal
AICAR
Basal
AICAR
c
Palmitate oxidation
(μmol min-1 mg-1)
1.5
1.0
0.5
0.0
†
P=0.06
***
Basal
AICAR
Basal
AICAR
d
Fat utilisation (%)
60
40
20
0
†
*
Saline
AICAR
Saline
AICAR
e
WT
KI
WT
KI
AICAR
- + - + - + - +
ACC2-p S212
ACC
ACC2-p S212/ ACC
(fold vs WT basal)
3
2
1
0
††
***
ND
ND
Basal
AICAR
Basal
AICAR

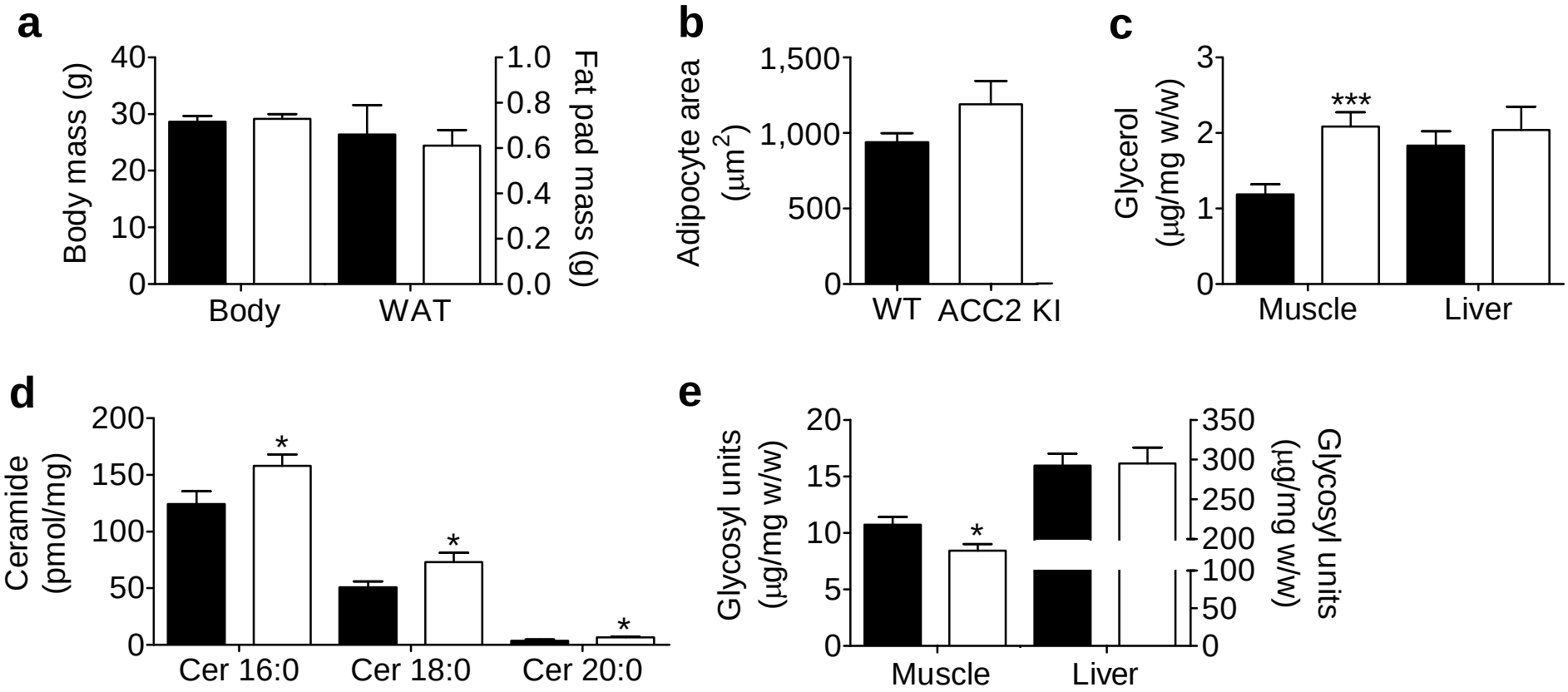
a
Body mass (g)
40
30
20
10
0
1.0
0.8
0.6
0.4
0.2
0.0
Fat pad mass (g)
Body
WAT
b
Adipocyte area (μm2)
1,500
1,000
500
0
WT
ACC2 KI
c
Glycerol (μg/mg w/w)
3
2
1
0
***
Muscle
Liver
d
Ceramide (pmol/mg)
200
150
100
50
0
*
*
*
Cer 16:0
Cer 18:0
Cer 20:0
e
Glycosyl units (μg/mg w/w)
20
15
10
5
0
*
350
300
250
200
100
50
0
Glycosyl units (μg/mg w/w)
Muscle
Liver

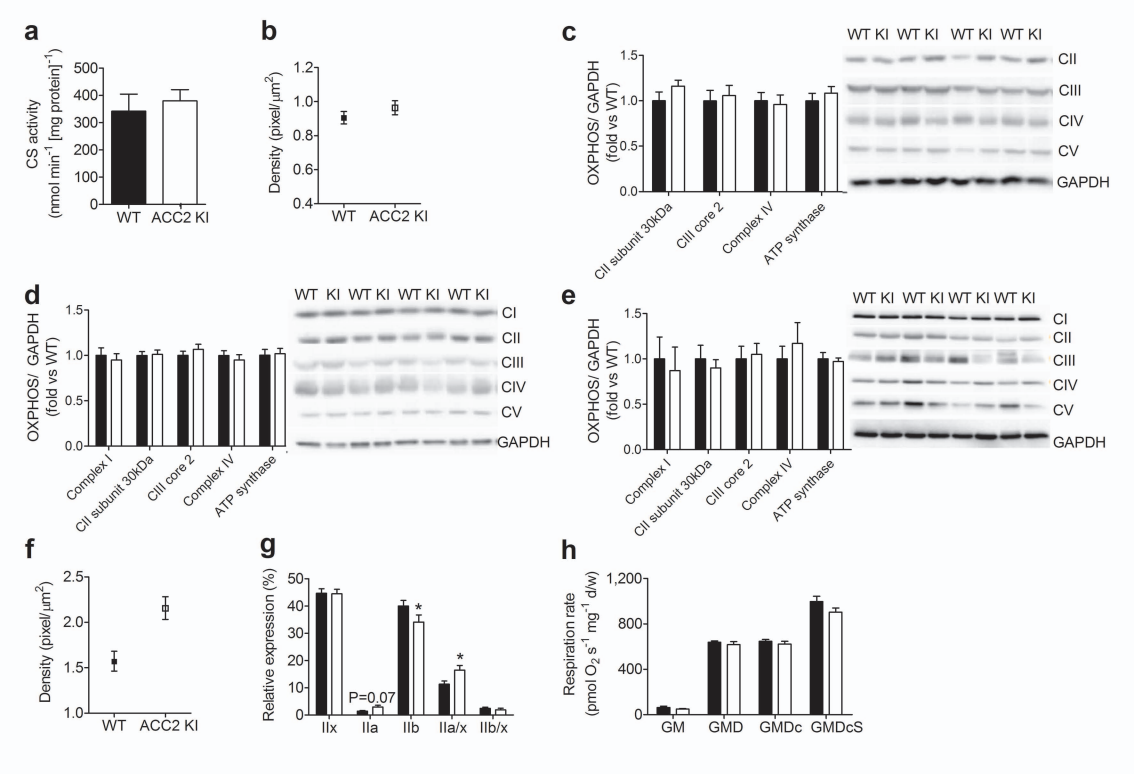
a
CS activity (nmol min-1 [mg protein]-1)
500
400
300
200
100
0
WT
ACC2 KI
b
Density (pixel/µm2)
1.2
1.0
0.8
0.6
0.4
WT
ACC2 KI
c
WT KI WT KI WT KI WT KI
OXPHOS/ GAPDH (fold vs WT)
1.5
1.0
0.5
0.0
CII
CIII
CIV
CV
GAPDH
CII subunit 30kDa
CIII core 2
Complex IV
ATP synthase
d
WT KI WT KI WT KI WT KI
OXPHOS/ GAPDH (fold vs WT)
CI
CII
CIII
CIV
CV
GAPDH
Complex I
CII subunit 30kDa
CIII core 2
Complex IV
ATP synthase
e
WT KI WT KI WT KI WT KI
OXPHOS/ GAPDH (fold vs WT)
CI
CII
CIII
CIV
CV
GAPDH
Complex I
CII subunit 30kDa
CIII core 2
Complex IV
ATP synthase
f
Density (pixel/µm2)
2.5
2.0
1.5
1.0
WT
ACC2 KI
g
Relative expression (%)
50
40
30
20
10
0
P=0.07
*
*
IIx
IIa
IIb
IIa/x
IIb/x
h
Respiration rate (pmol O2 s-1 mg-1 d/w)
1,200
800
400
0
GM
GMD
GMDc
GMDcS

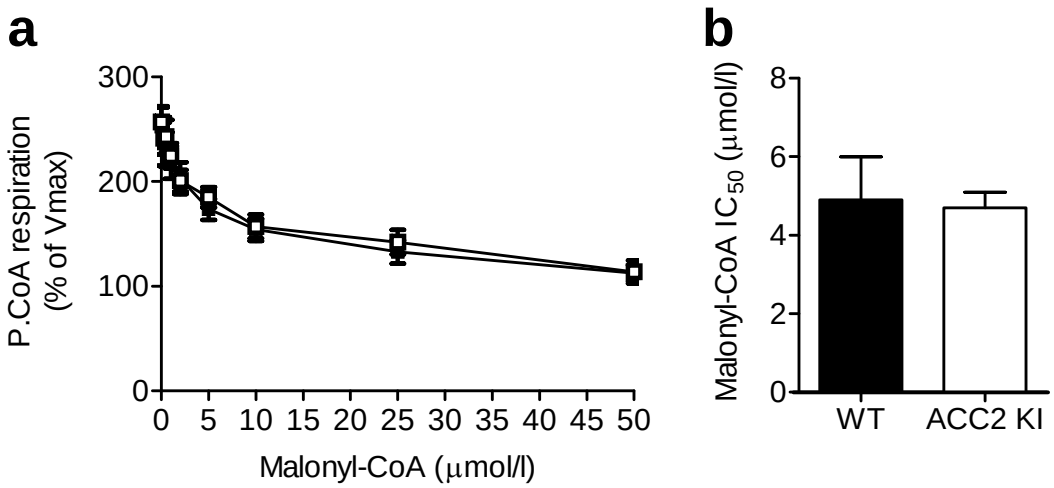
a
P.CoA respiration
(% of Vmax)
300
200
100
0
0 5 10 15 20 25 30 35 40 45 50
Malonyl-CoA (µmol/l)

b
Malonyl-CoA IC50 (µmol/l)
8
6
4
2
0
WT
ACC2 KI

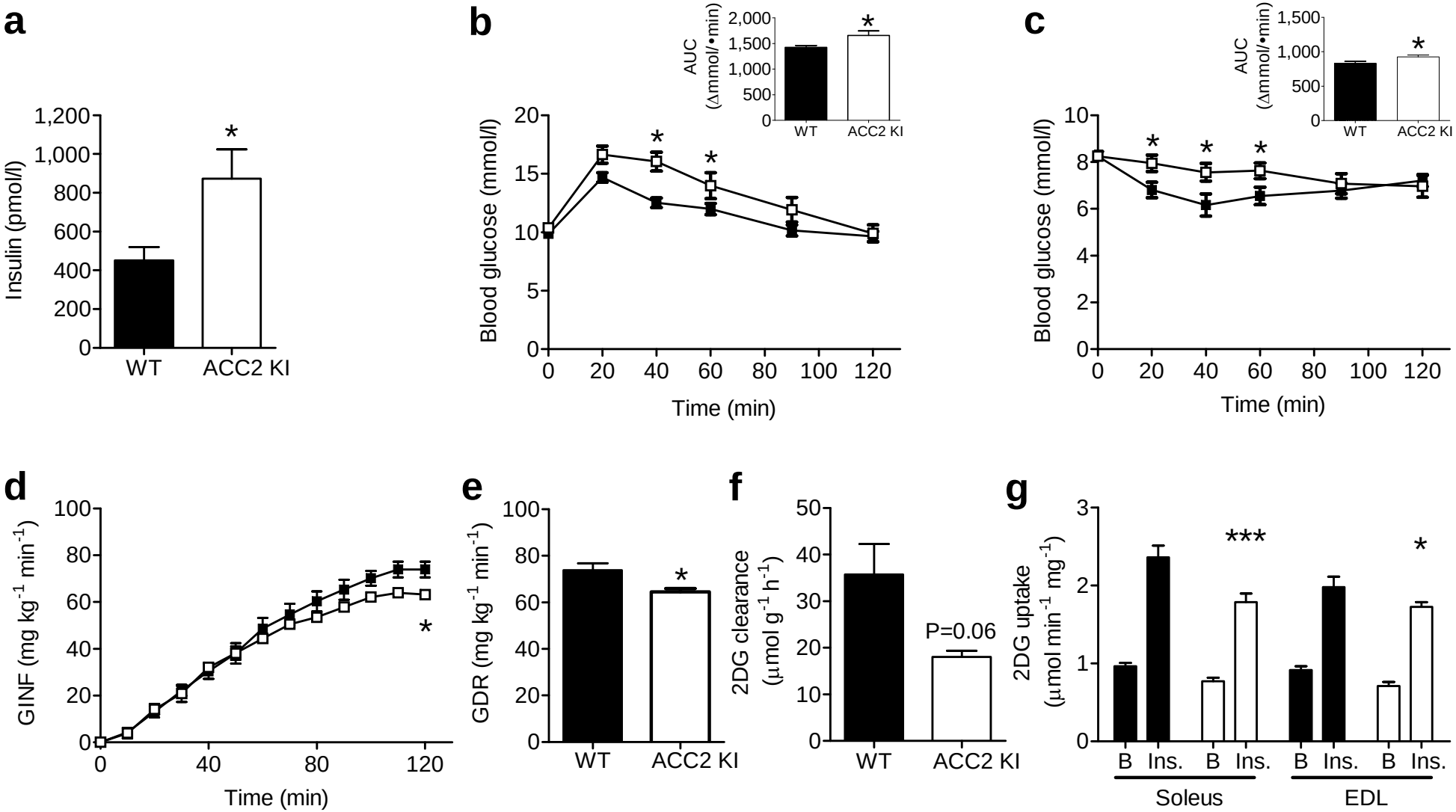
a
Insulin (pmol/l)
1,200
1,000
800
600
400
200
0
*
WT
ACC2 KI
b
Blood glucose (mmol/l)
20
15
10
5
0
0 20 40 60 80 100 120
Time (min)
*
*
AUC (Δmmol/•min)
2,000
1,500
1,000
500
0
*
WT
ACC2 KI
c
Blood glucose (mmol/l)
10
8
6
4
2
0
0 20 40 60 80 100 120
Time (min)
*
*
*
AUC (Δmmol/•min)
1,500
1,000
500
0
*
WT
ACC2 KI
d
GINF (mg kg-1 min-1)
100
80
60
40
20
0
0 40 80 120
Time (min)
*
e
GDR (mg kg-1 min-1)
100
80
60
40
20
0
*
WT
ACC2 KI
f
2DG clearance (µmol g-1 h-1)
50
40
30
20
10
0
P=0.06
WT
ACC2 KI
g
2DG uptake (µmol min-1 mg-1)
3
2
1
0
***
*
B Ins. B Ins. B Ins. B Ins.
Soleus
EDL

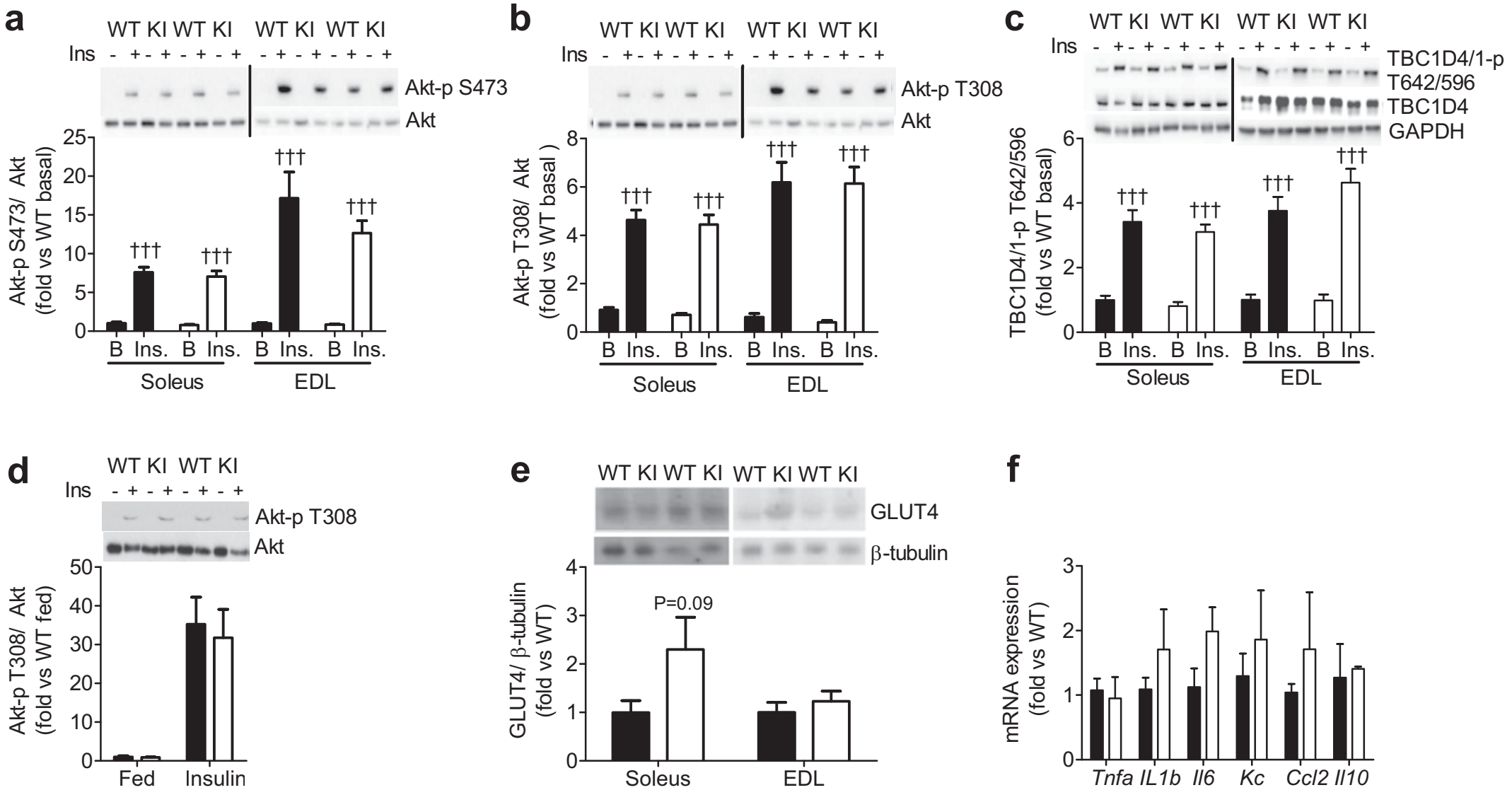
a
WT KI WT KI WT KI WT KI
Ins - + - + - + - + - + - + - + - +
Akt-p S473
Akt
Akt-p S473/ Akt
(fold vs WT basal)
25
20
15
10
5
0
†††
†††
†††
†††
B Ins. B Ins. B Ins. B Ins.
Soleus
EDL
b
WT KI WT KI WT KI WT KI
Ins - + - + - + - + - + - + - + - +
Akt-p T308
Akt
Akt-p T308/ Akt
(fold vs WT basal)
8
6
4
2
0
†††
†††
†††
†††
B Ins. B Ins. B Ins. B Ins.
Soleus
EDL
c
WT KI WT KI WT KI WT KI
Ins - + - + - + - + - + - + - + - +
TBC1D4/1-p
T642/596
TBC1D4
GAPDH
TBC1D4/1-p T642/596
(fold vs WT basal)
6
4
2
0
†††
†††
†††
†††
B Ins. B Ins. B Ins. B Ins.
Soleus
EDL
d
WT KI WT KI
Ins - + - + - + - +
Akt-p T308
Akt
Akt-p T308/ Akt
(fold vs WT fed)
50
40
30
20
10
0
Fed
Insulin
e
WT KI WT KI WT KI WT KI
GLUT4
β-tubulin
GLUT4/ β-tubulin
(fold vs WT)
4
3
2
1
0
P=0.09
Soleus
EDL
f
mRNA expression
(fold vs WT)
3
2
1
0
Tnfa IL1b Il6 Kc Ccl2 Il10

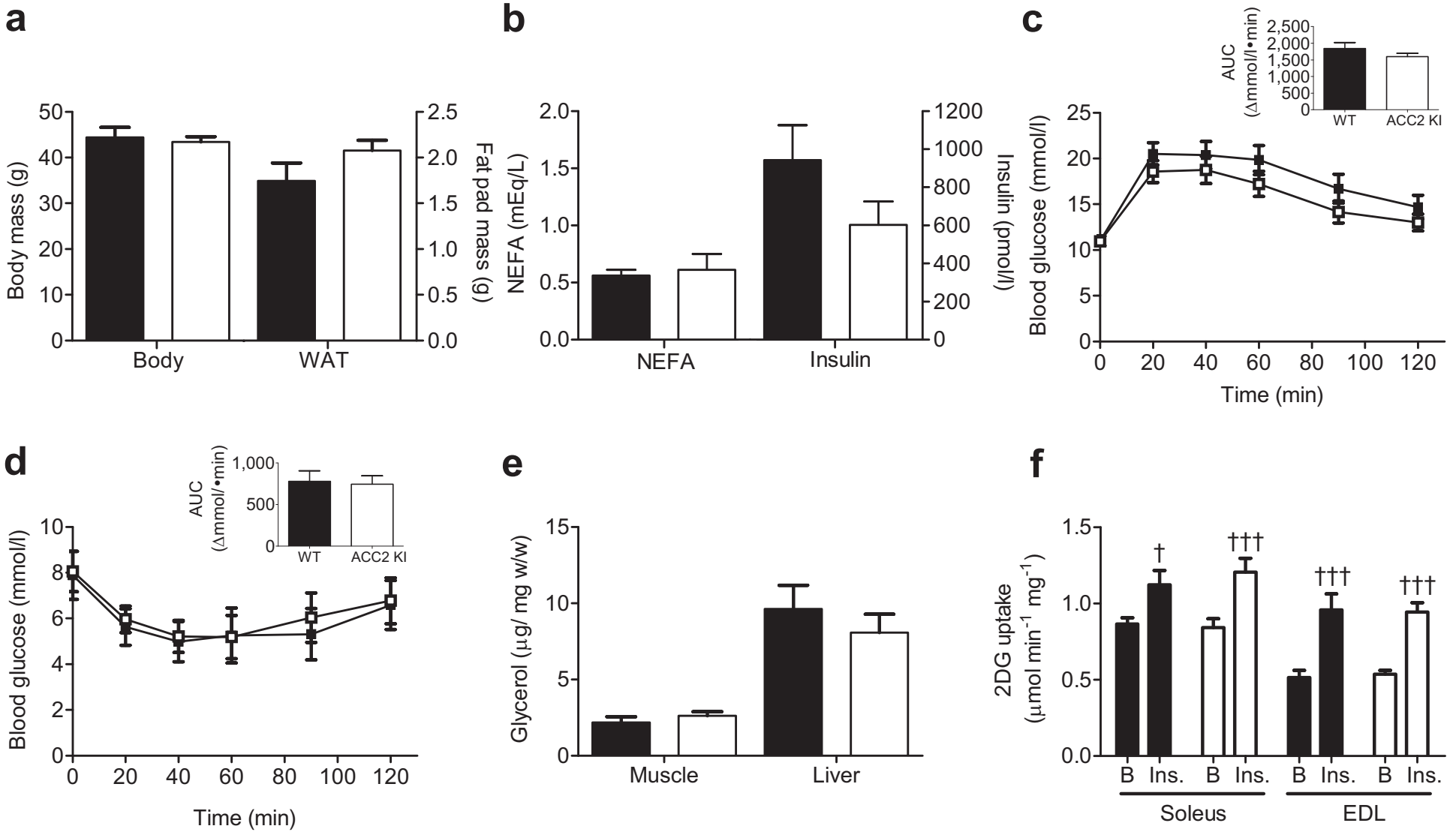
a
Body mass (g)
Fat pad mass (g)
Body
WAT
b
NEFA (mEq/L)
Insulin (pmol/l)
NEFA
Insulin
c
AUC (Δmmol/l•min)
WT
ACC2 KI
Blood glucose (mmol/l)
Time (min)
d
AUC (Δmmol/•min)
WT
ACC2 KI
Blood glucose (mmol/l)
Time (min)
e
Glycerol (µg/ mg w/w)
Muscle
Liver
f
2DG uptake (µmol min-1 mg-1)
B
Ins.
Soleus
EDL

14 0248
O'Neill
Fig. 1

Global: No bold except fig. part labels.

Please set in 2/3 page

14 0248
Fig. 2

No bold except part labels

Set in 10·5cm

14 0248
Fig. 3

No bold except part labels

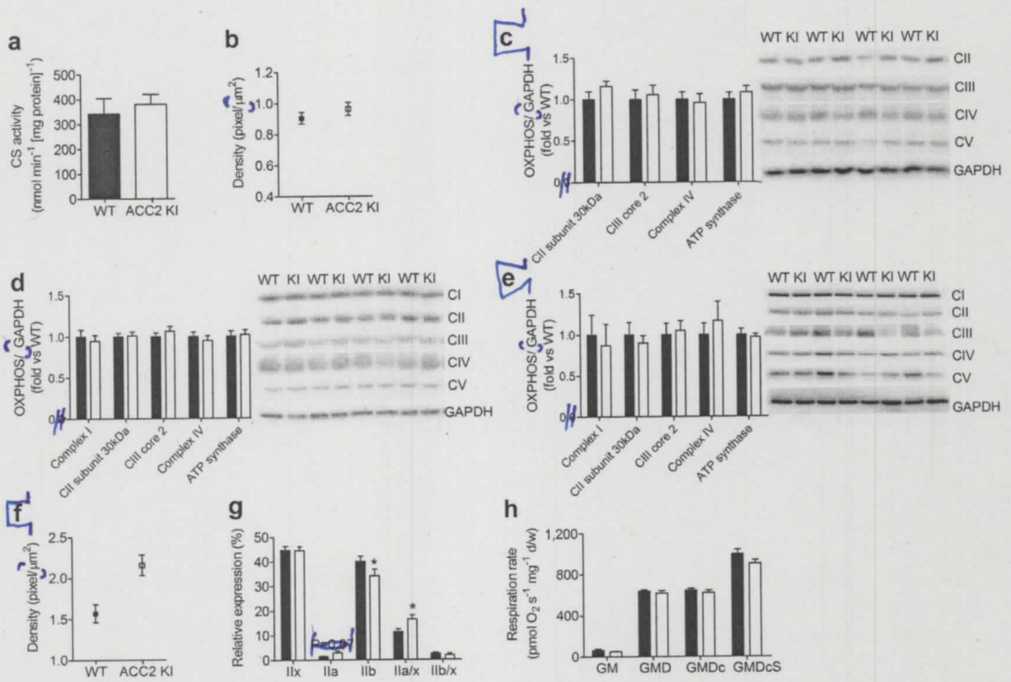

Set in 14 cm

14 0248
Fig. 4

overdot
$\dot{V}_{max}$

No bold except part labels

Set in 7·5 cm

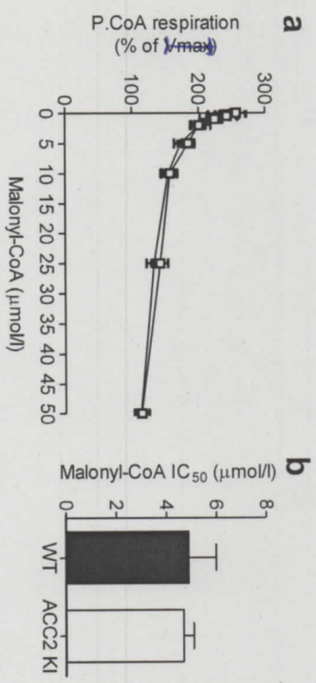

14 0248
Fig. 5

No bold except part labels

Set in 15cm

Gk. cap. delta
↓
Δ mmol/l × min (x2)
↓
Mult.

of
of (x4)

140248
Fig. 6

No bold except part labels

Set in 15·5 cm

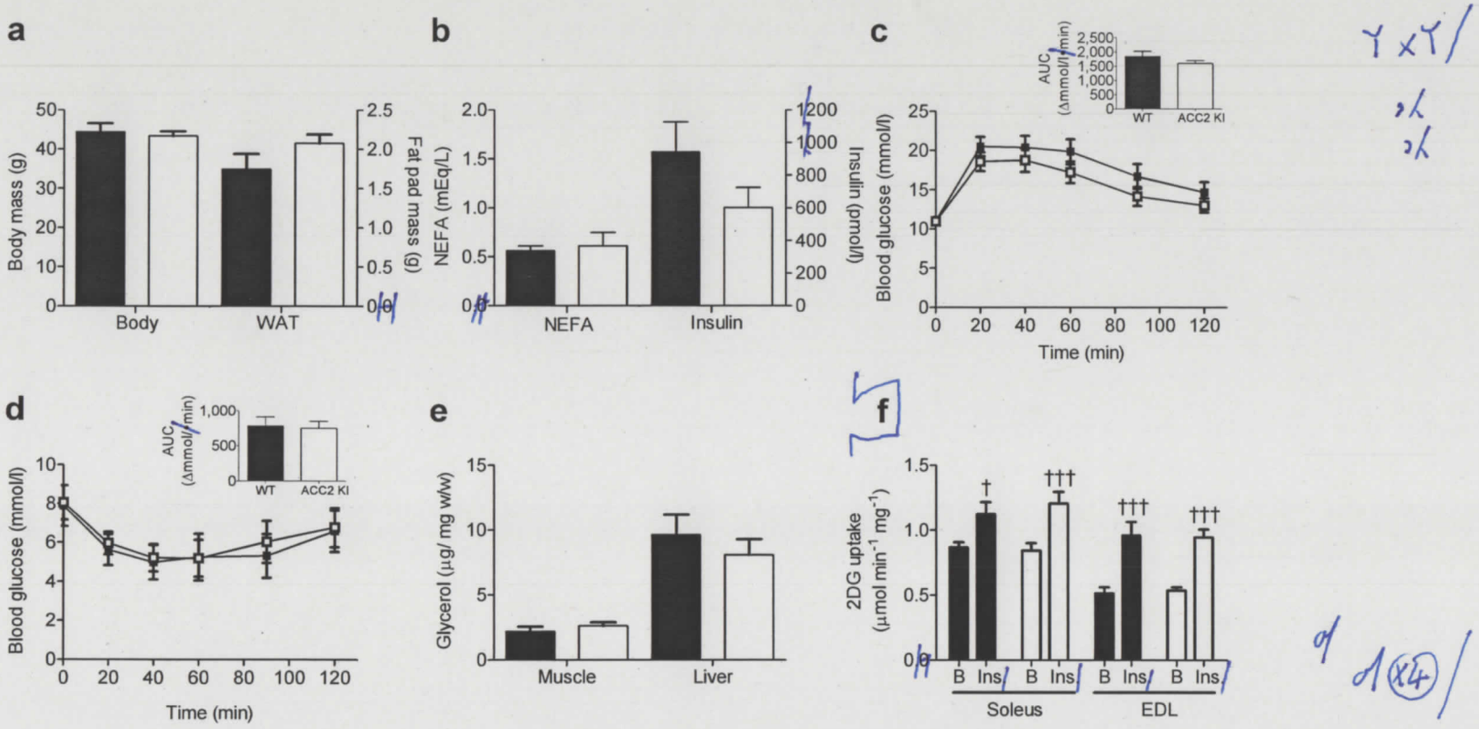

14/02/48
Fig. 7

No bold except part labels

Set in 15cm